

*Supporting Information for*

# **Valence Tautomerism in Chromium Half-Sandwich Triarylmethylium Dyads**

**Anja Rehse, Michael Linseis, Mykhailo Azarkh, Malte Drescher and Rainer F. Winter \***

Department of Chemistry, Universität Konstanz, Universitätsstraße 10, 78464 Konstanz, Germany

\* Correspondence: rainer.winter@uni-konstanz.de

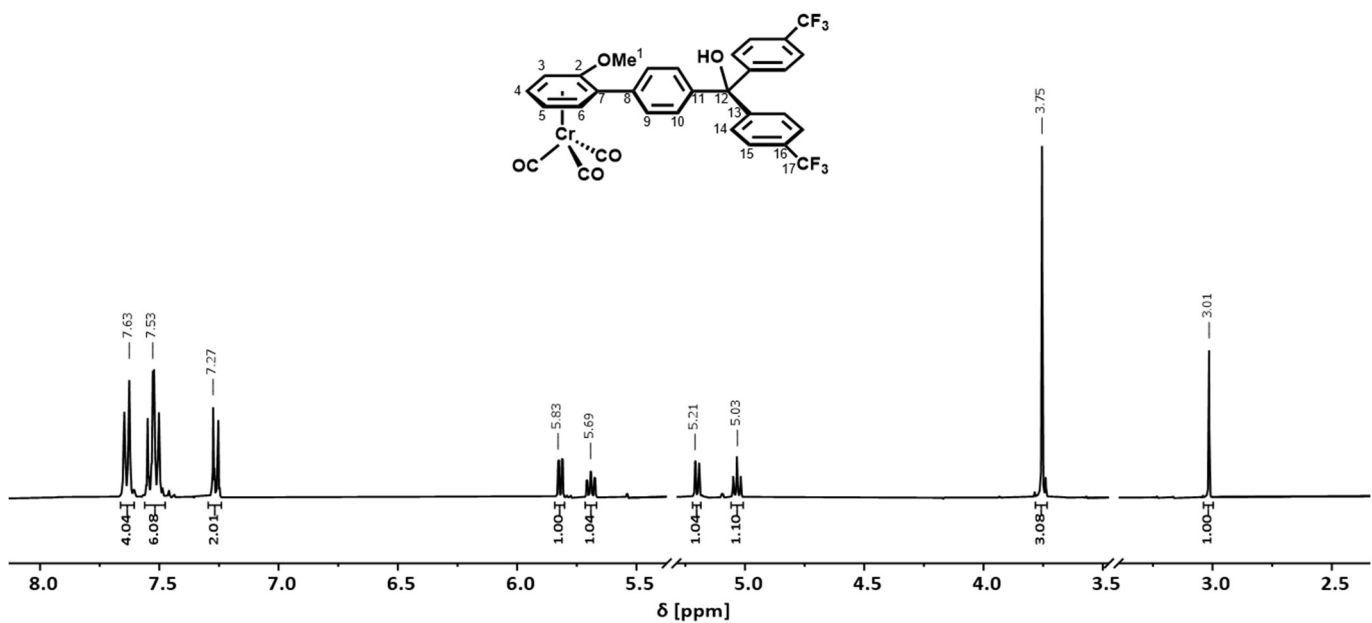


**Figure S1.**  $^1\text{H}$ -NMR spectrum of complex **1-OH** (400 MHz,  $\text{CD}_2\text{Cl}_2$ ).

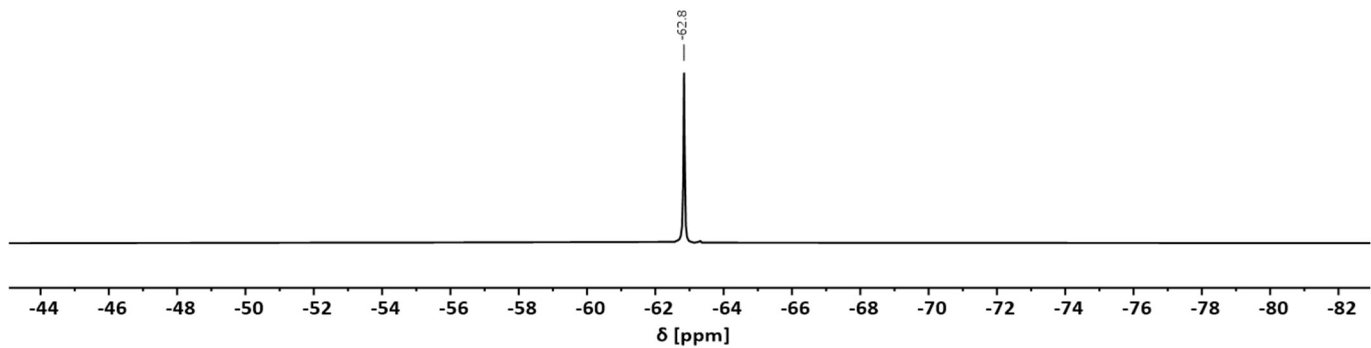


**Figure S2.**  $^{19}\text{F}\{^1\text{H}\}$ -NMR spectrum of complex **1-OH** (376 MHz,  $\text{CD}_2\text{Cl}_2$ ).

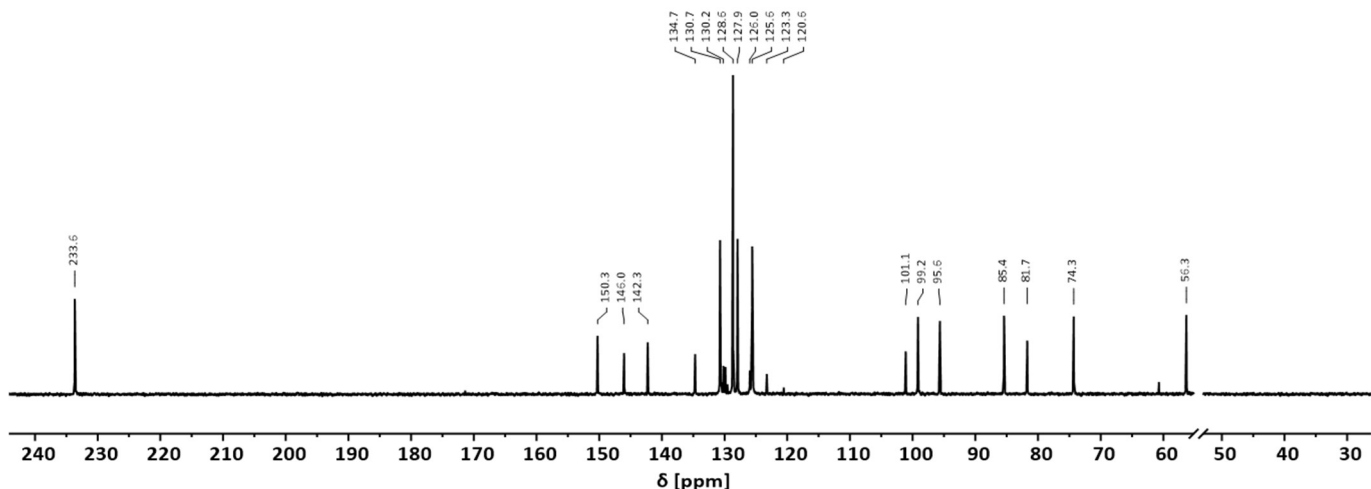


**Figure S3.**  $^{13}\text{C}\{^1\text{H}\}$ -NMR spectrum of complex **1-OH** (101 MHz,  $\text{CD}_2\text{Cl}_2$ ).

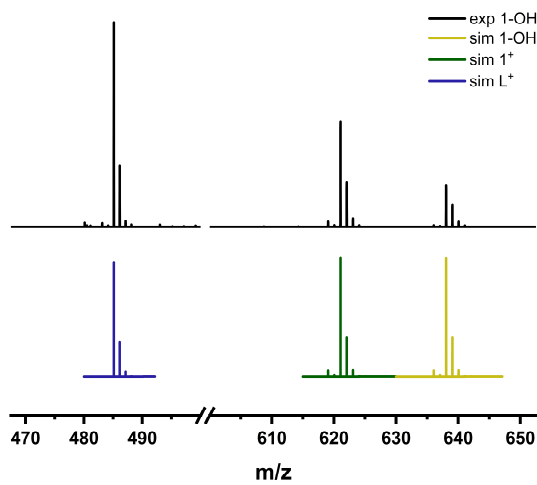


**Figure S4.** Experimental (black) and simulated (carbinol yellow, tritylium complex green, tritylium ligand blue) mass spectrum of complex **1-OH**.

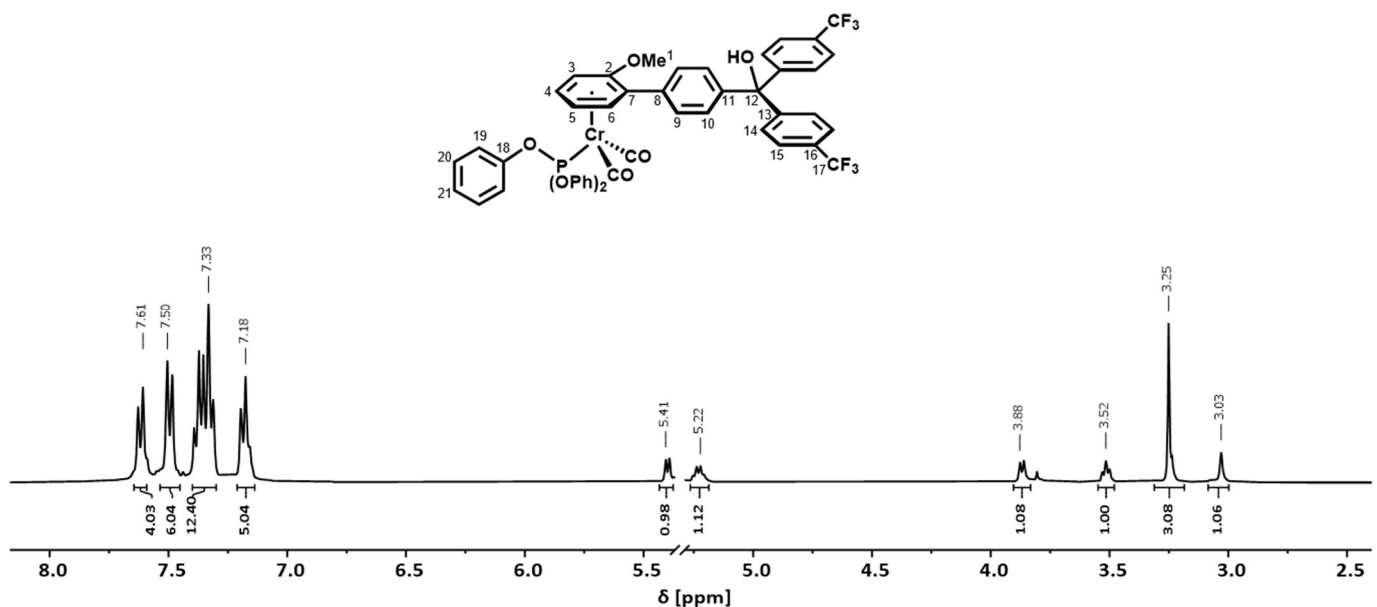


**Figure S5.**  $^1\text{H}$ -NMR spectrum of complex **2-OH** (400 MHz,  $\text{CD}_2\text{Cl}_2$ ).

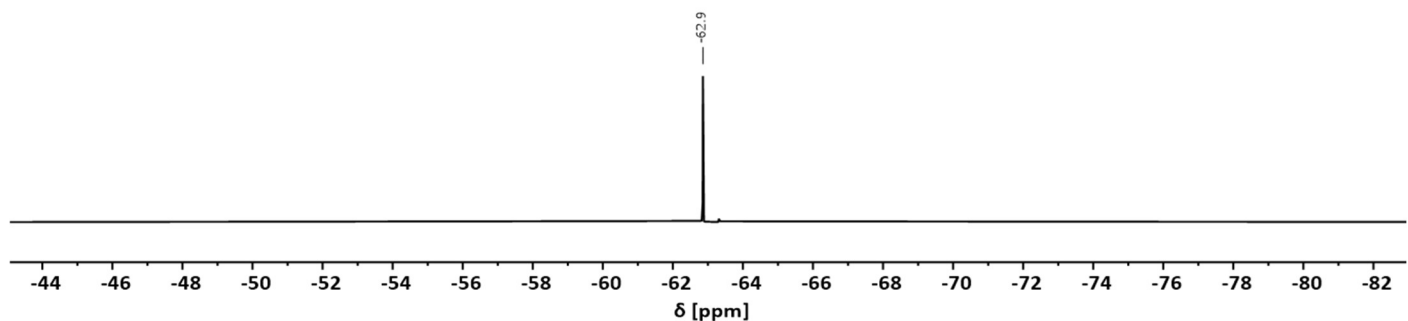


**Figure S6.**  $^{19}\text{F}\{^1\text{H}\}$ -NMR spectrum of complex **2-OH** (376 MHz,  $\text{CD}_2\text{Cl}_2$ ).

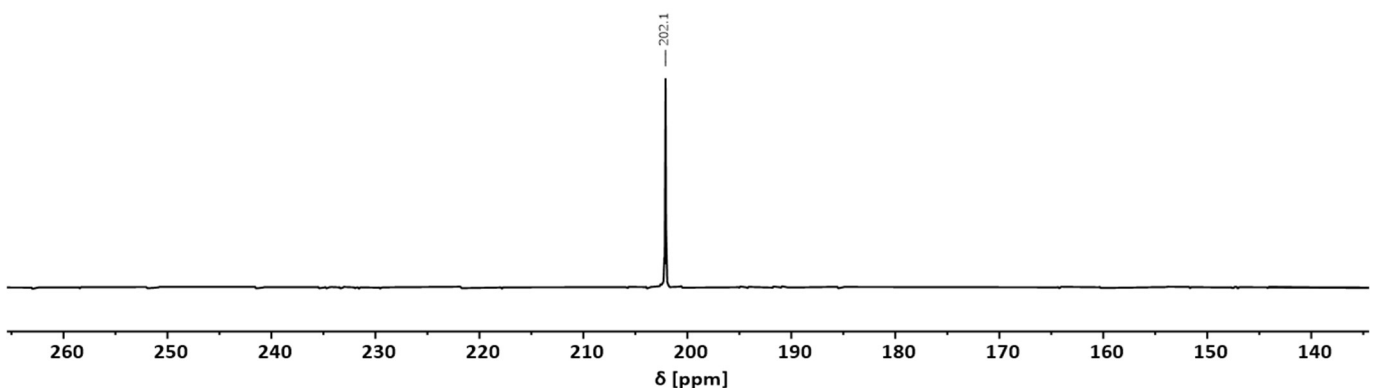


**Figure S7.**  $^{31}\text{P}\{\text{H}\}$ -NMR spectrum of complex 2-OH (162 MHz,  $\text{CD}_2\text{Cl}_2$ ).

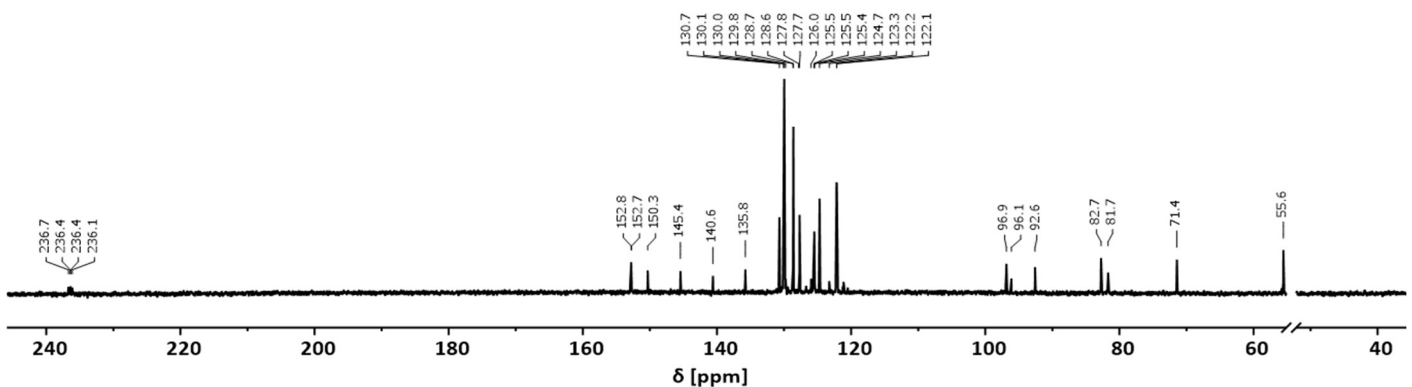


**Figure S8.**  $^{13}\text{C}\{\text{H}\}$ -NMR spectrum of complex 2-OH (101 MHz,  $\text{CD}_2\text{Cl}_2$ ).

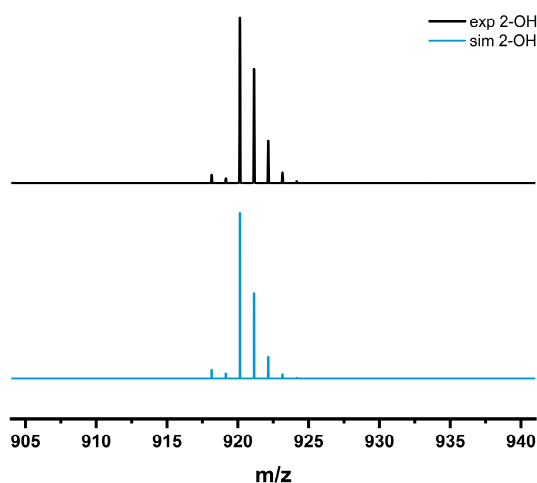


**Figure S9.** Experimental (black) and simulated (blue) mass spectrum of complex 2-OH.

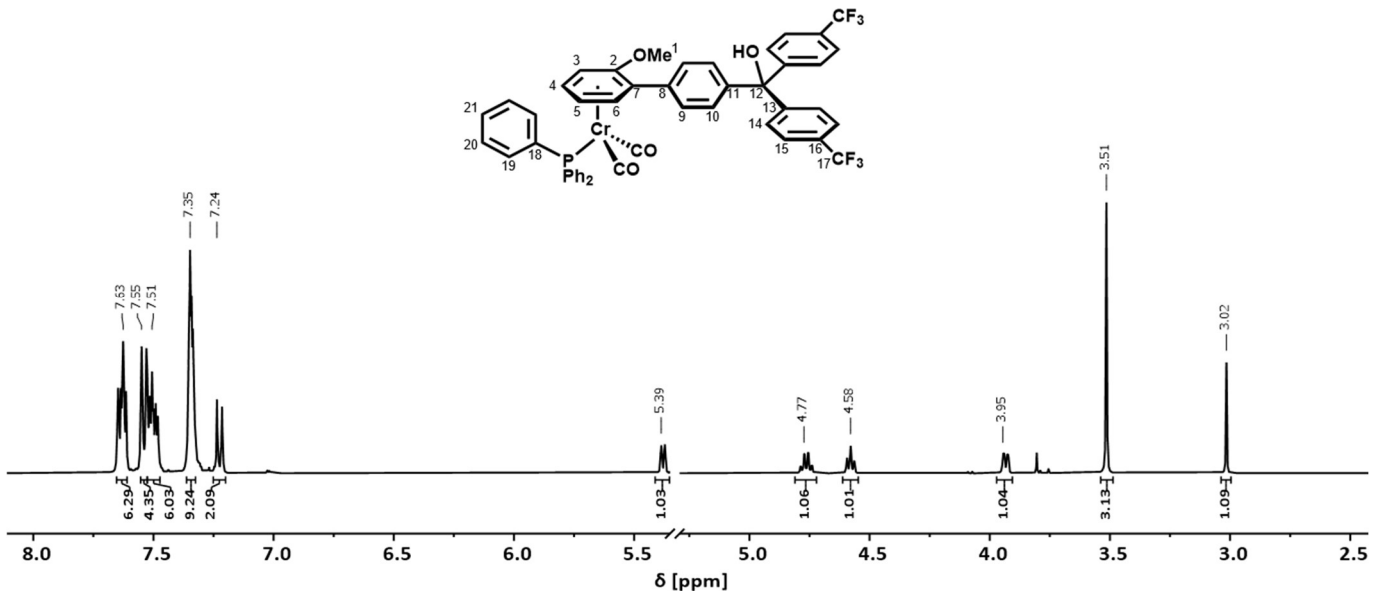


Figure S10.  $^1\text{H}$ -NMR spectrum of complex  $\text{3-OH}$  (400 MHz,  $\text{CD}_2\text{Cl}_2$ ).

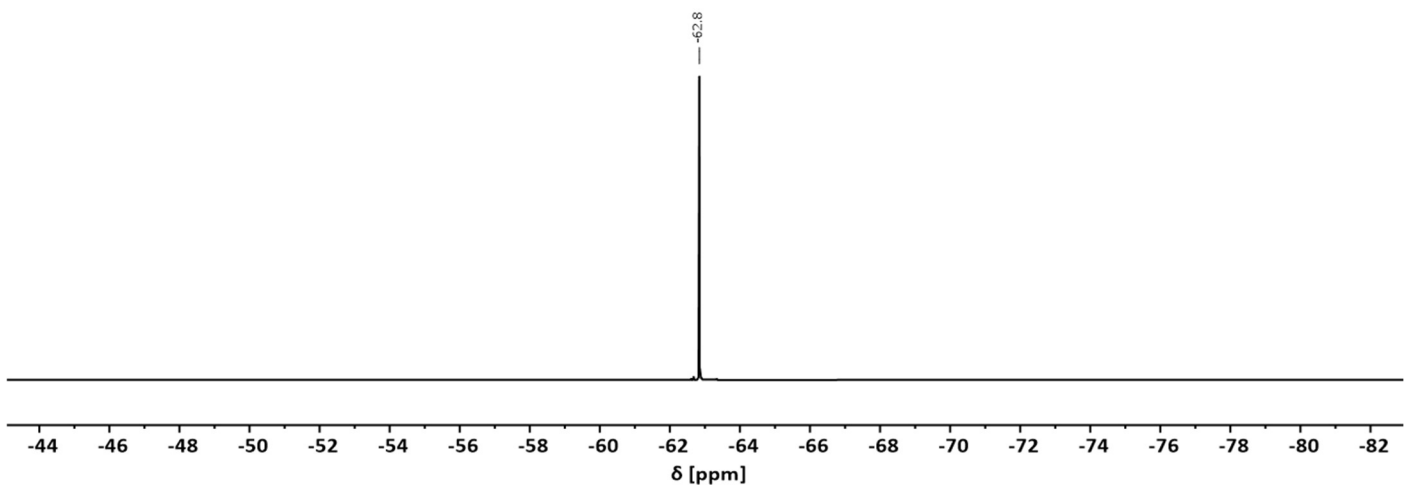


Figure S11.  $^{19}\text{F}\{^1\text{H}\}$ -NMR spectrum of complex  $\text{3-OH}$  (376 MHz,  $\text{CD}_2\text{Cl}_2$ ).

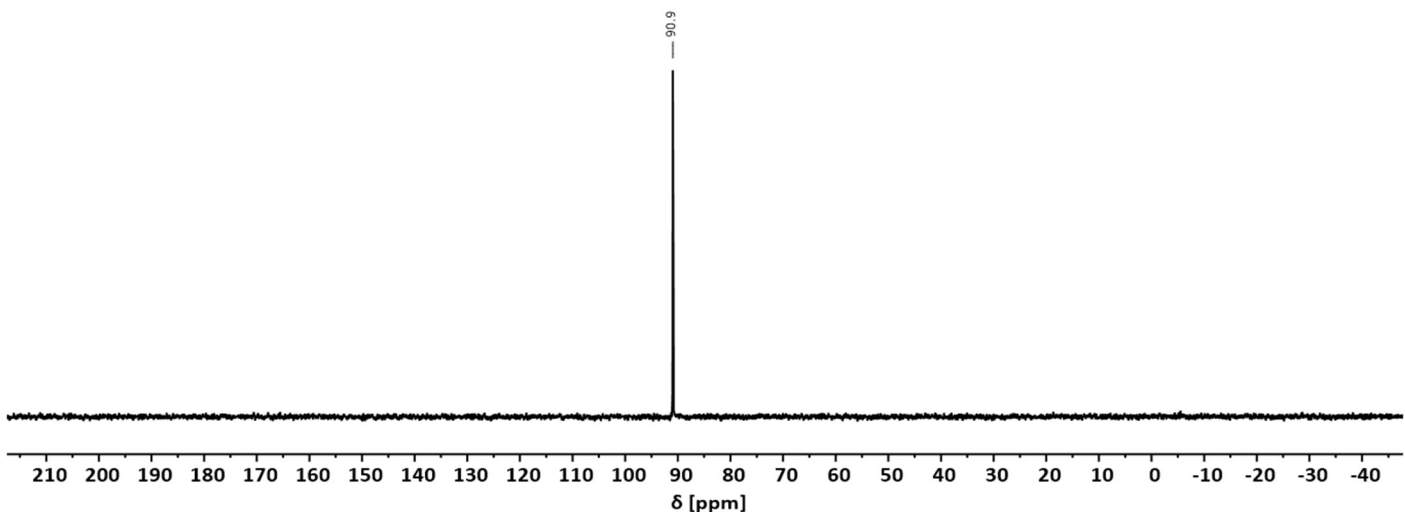
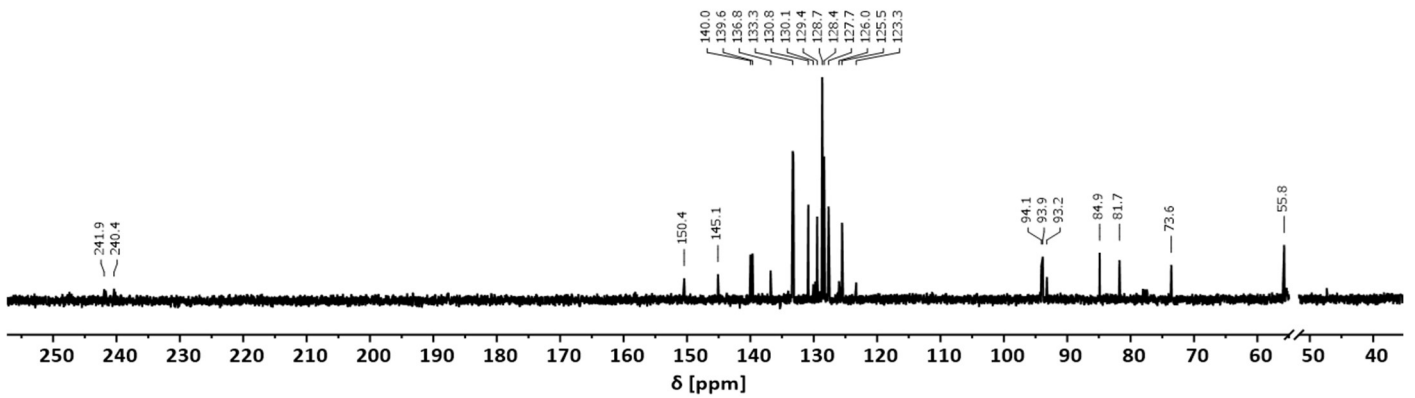
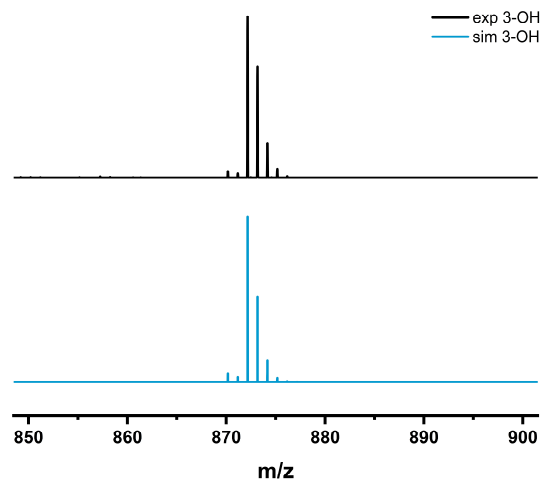


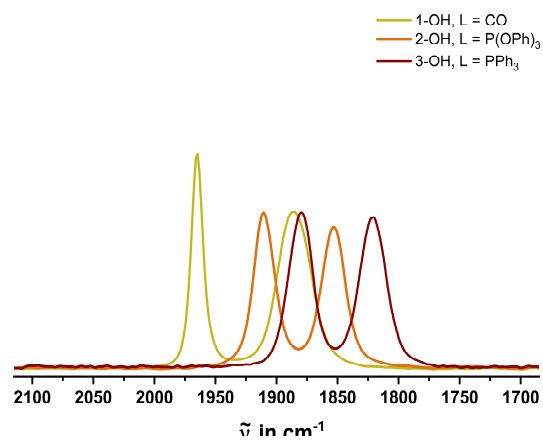
Figure S12.  $^{31}\text{P}\{^1\text{H}\}$ -NMR spectrum of complex  $\text{3-OH}$  (162 MHz,  $\text{CD}_2\text{Cl}_2$ ).



**Figure S13.**  $^{13}\text{C}^{\{1\text{H}\}}$ -NMR spectrum of complex 3-OH (101 MHz,  $\text{CD}_2\text{Cl}_2$ ).



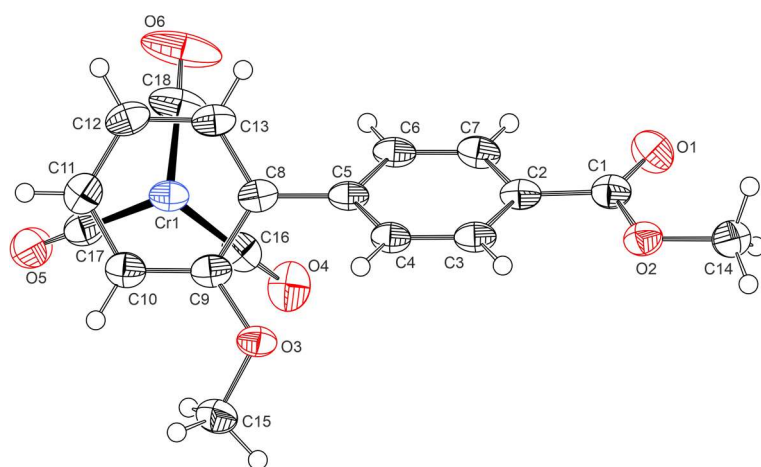
**Figure S14.** Experimental (black) and simulated (blue) mass spectrum of complex 3-OH.



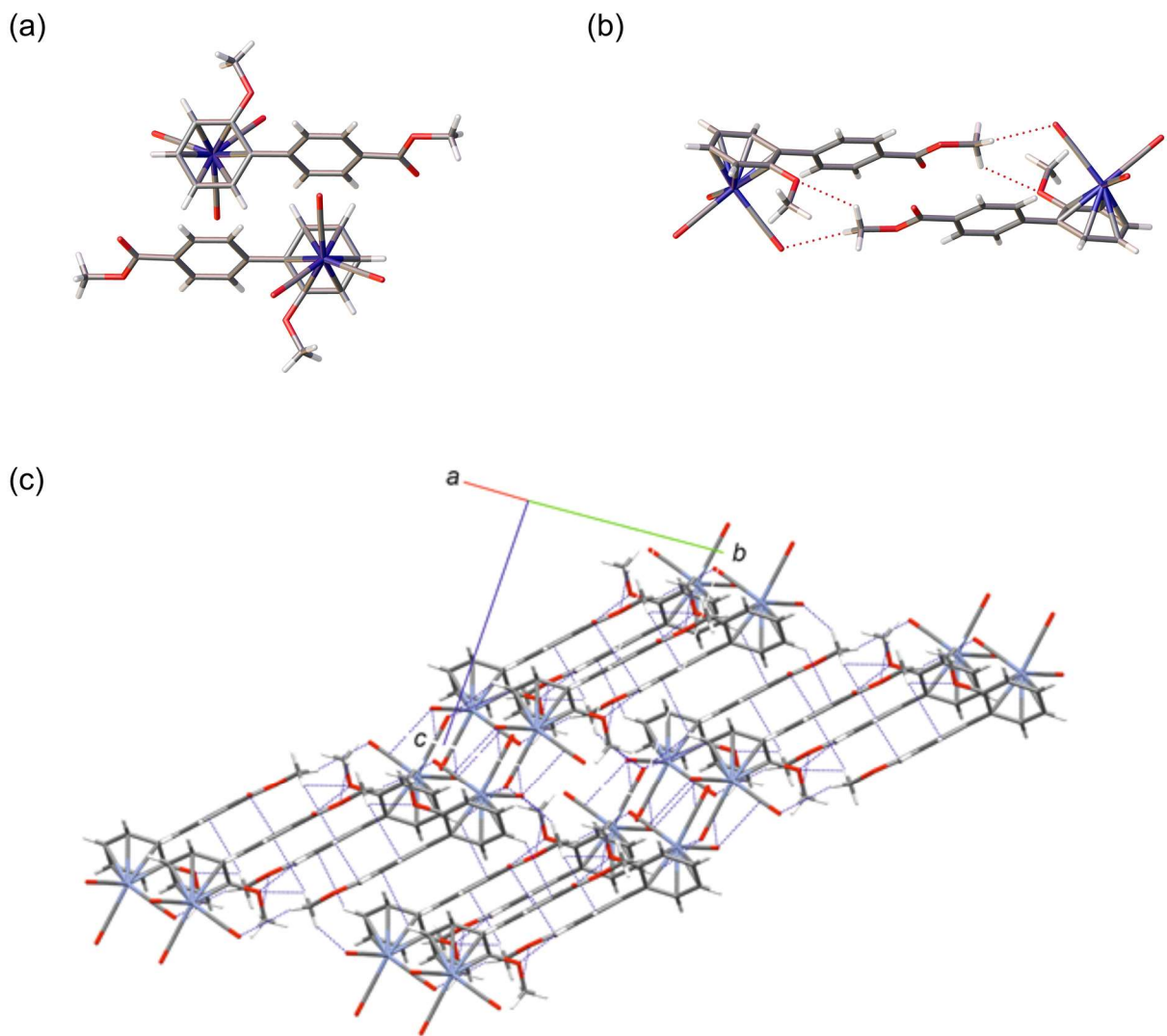
**Figure S15.** CO stretching vibrations in the IR spectra of complexes 1-OH-3-OH in  $\text{CH}_2\text{Cl}_2$ .

**Table S1.** Crystal data and structure refinement for [(biaryl-ester)Cr(CO)<sub>3</sub>] **1'**.

Empirical formula	CrC <sub>18</sub> O <sub>6</sub> H <sub>14</sub>
Formula weight	378.29
Temperature / K	100
Crystal system	triclinic
Space group	<i>P</i> -1
<i>a</i> / Å	7.3806(8)
<i>b</i> / Å	9.6181(9)
<i>c</i> / Å	12.1058(12)
$\alpha$ / °	100.346(8)
$\beta$ / °	105.803(8)
$\gamma$ / °	92.640(8)
Volume / Å <sup>3</sup>	809.33(15)
<i>Z</i>	2
$\rho_{\text{calc}}/\text{g cm}^{-3}$	1.552
$\mu/\text{mm}^{-1}$	0.739
<i>F</i> (000)	388.0
Crystal size / mm <sup>3</sup>	0.2 × 0.2 × 0.2
Radiation	Mo K $\alpha$ ( $\lambda = 0.71073$ )
2 $\Theta$ range for data collection / °	5.766 to 55.196
Index ranges	-9 ≤ <i>h</i> ≤ 9, -12 ≤ <i>k</i> ≤ 12, -15 ≤ <i>l</i> ≤ 15
Reflections collected	9772
Independent reflections	3726 [ $R_{\text{int}} = 0.0413$ , $R_{\text{sigma}} = 0.0331$ ]
Data/restraints/parameters	3726/0/229
Goodness-of-fit on <i>F</i> <sup>2</sup>	1.053
Final <i>R</i> indexes [ <i>I</i> ≥ 2 $\sigma$ ( <i>I</i> )]	$R_1 = 0.0714$ , $wR_2 = 0.1894$
Final <i>R</i> indexes [all data]	$R_1 = 0.0809$ , $wR_2 = 0.2049$
Largest diff. peak/hole / e Å <sup>-3</sup>	1.86/-1.16



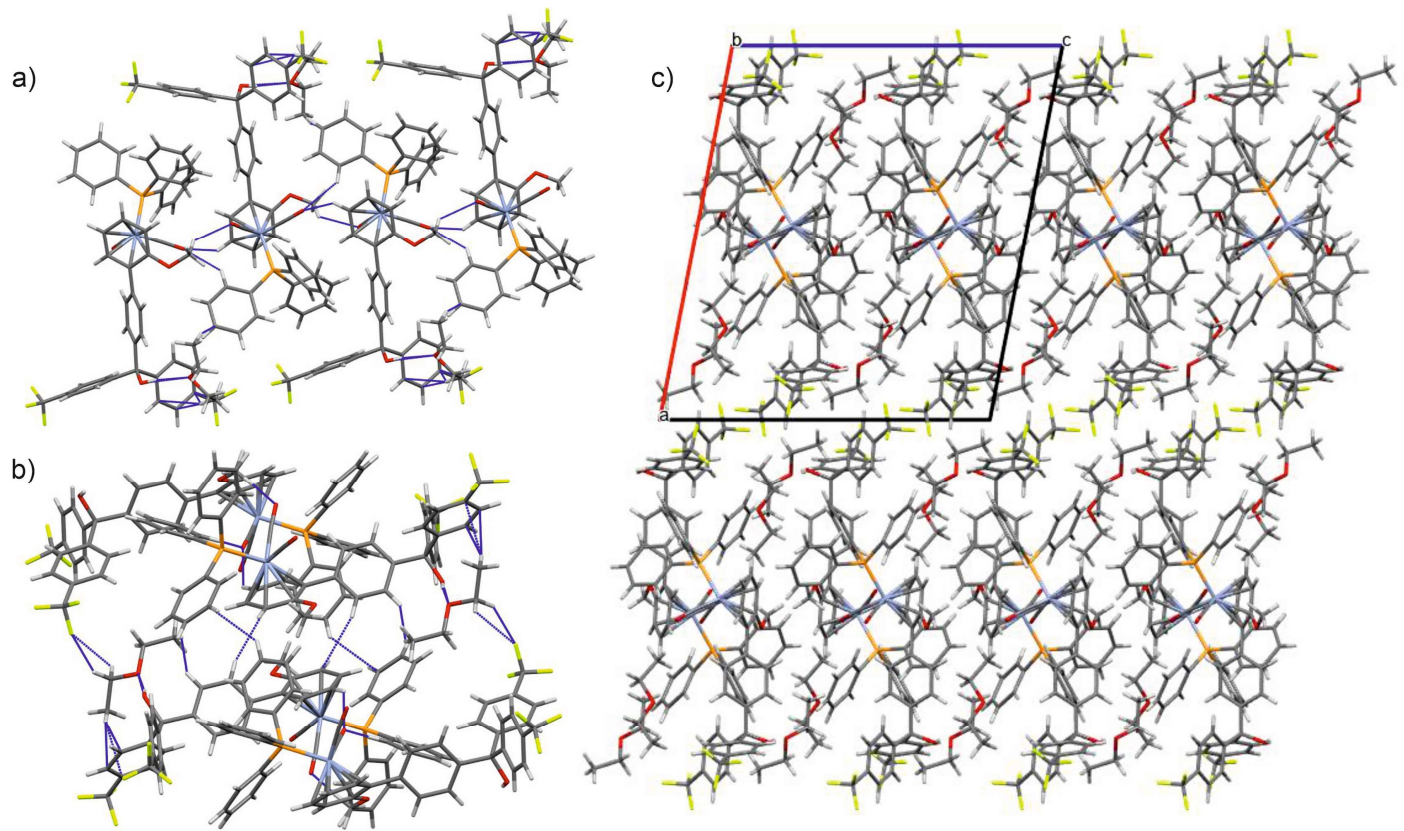
**Figure S16.** ORTEP of the *S*<sub>P</sub> enantiomer of [(biaryl-ester)Cr(CO)<sub>3</sub>], complex **1'**, with the atomic numbering. Ellipsoids are displayed at the 50% probability level.



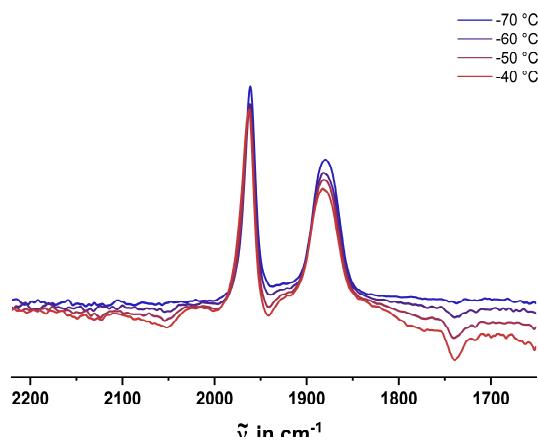
**Figure S17.** (a) The two enantiomers within the unit cell of **1'**. (b) Tail-to-tail dimers of **1'**. (c) Packing of **1'** in the crystal. Short contacts are indicated by blue and red broken lines, respectively.

**Table S2.** Crystal data and structure refinement for 3-OH.

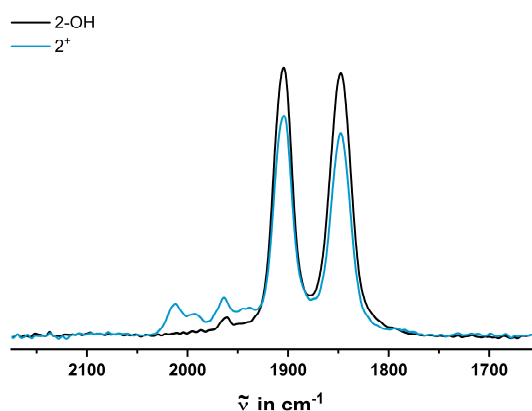
Empirical formula	C <sub>56</sub> H <sub>55</sub> CrF <sub>6</sub> O <sub>6</sub> P
Formula weight	1020.97
Temperature / K	100
Crystal system	monoclinic
Space group	<i>P</i> 2 <sub>1</sub> /c
<i>a</i> / Å	20.7617(8)
<i>b</i> / Å	13.7170(3)
<i>c</i> / Å	17.9942(7)
$\alpha$ / °	90
$\beta$ / °	101.005(3)
$\gamma$ / °	90
Volume / Å <sup>3</sup>	5030.3(3)
<i>Z</i>	4
$\rho_{\text{calc}}$ g / cm <sup>3</sup>	1.348
$\mu$ / mm <sup>-1</sup>	0.332
<i>F</i> (000)	2128.0
Crystal size / mm <sup>3</sup>	0.4 × 0.267 × 0.2
Radiation	Mo K $\alpha$ ( $\lambda$ = 0.71073)
2 $\Theta$ range for data collection / °	4.612 to 51.912
Index ranges	-25 ≤ <i>h</i> ≤ 25, -16 ≤ <i>k</i> ≤ 16, -22 ≤ <i>l</i> ≤ 19
Reflections collected	22453
Independent reflections	9749 [ $R_{\text{int}} = 0.0401$ , $R_{\text{sigma}} = 0.0570$ ]
Data/restraints/parameters	9749/185/791
Goodness-of-fit on <i>F</i> <sup>2</sup>	1.033
Final <i>R</i> indexes [ <i>I</i> ≥ 2 $\sigma$ ( <i>I</i> )]	$R_1 = 0.0566$ , $wR_2 = 0.1327$
Final <i>R</i> indexes [all data]	$R_1 = 0.0974$ , $wR_2 = 0.1538$
Largest diff. peak/hole / e Å <sup>-3</sup>	0.47/-0.54



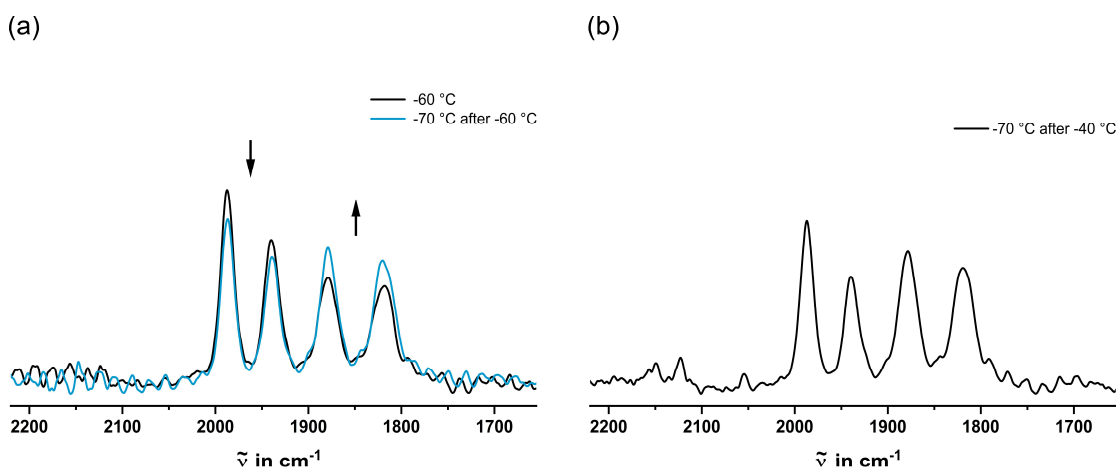
**Figure S18.** a) Chains of alternately aligned *R<sub>p</sub>/S<sub>p</sub>* enantiomers of **3-OH** with short intermolecular contacts indicated by blue broken lines progressing along the *b* axis of the unit cell. b) A view of two pairs of *R<sub>p</sub>/S<sub>p</sub>* enantiomers with the hydrogen-bonded ether solvent molecules. Short intermolecular contacts by C-H···π and C-H···F interactions are indicated by blue broken lines. c) Packing of the molecules within the unit cell as viewed along the *b* axis.



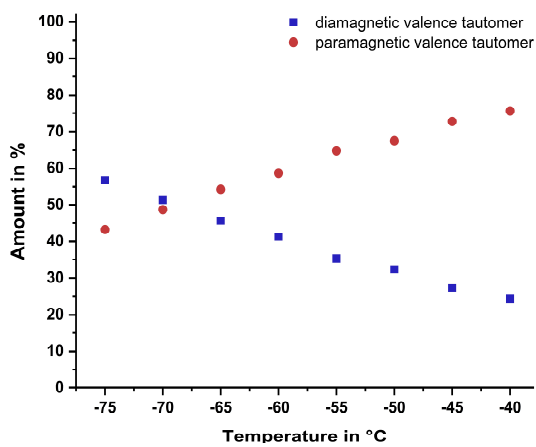
**Figure S19.** IR spectra of complex  $\mathbf{1}^+$  in  $\text{CH}_2\text{Cl}_2$  at temperatures between  $-70$  and  $-40$   $^\circ\text{C}$ .



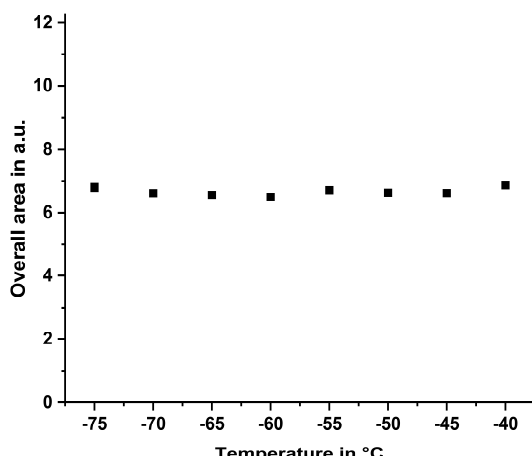
**Figure S20.** Baseline-corrected IR spectra of  $\mathbf{2}\text{-OH}$  and  $\mathbf{2}^+$  in  $\text{CH}_2\text{Cl}_2$  at  $-70$   $^\circ\text{C}$ .



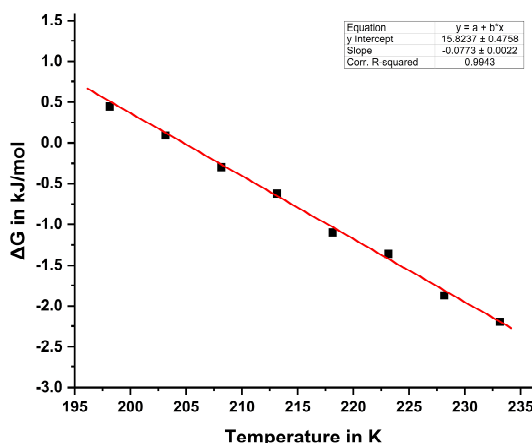
**Figure S21.** IR spectra of  $\mathbf{3}^+$  in  $\text{CH}_2\text{Cl}_2$  at (a)  $-70$  after warming to  $-60$   $^\circ\text{C}$ ; (b)  $-70$  after warming to  $-40$   $^\circ\text{C}$ .



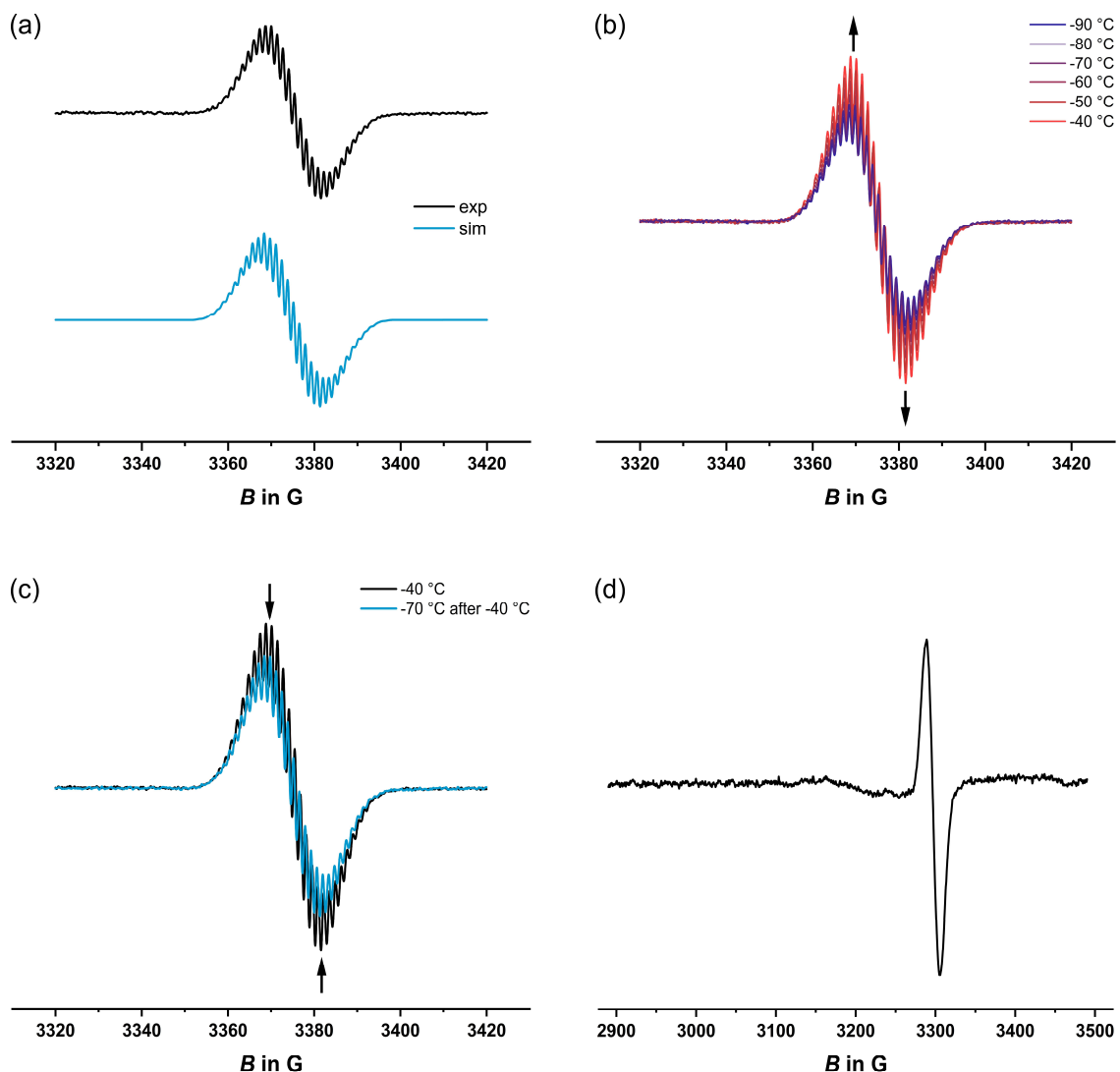
**Figure S22.** Amounts of the distinct valence tautomers of  $3^+$  between  $-70$  and  $-40$   $^{\circ}\text{C}$ .



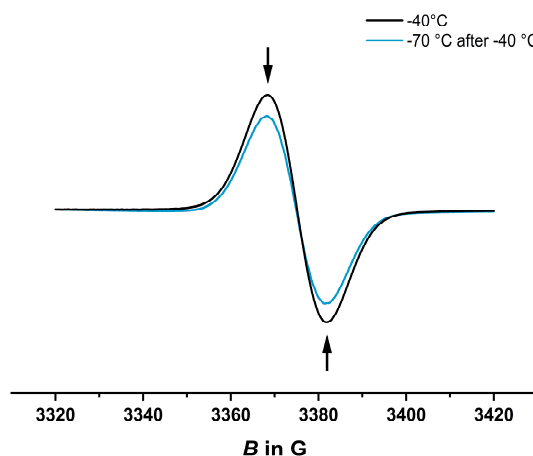
**Figure S23.** Total area of all carbonyl bands of complex  $3^+$  within the temperature range from  $-70$  to  $-40$   $^{\circ}\text{C}$ .



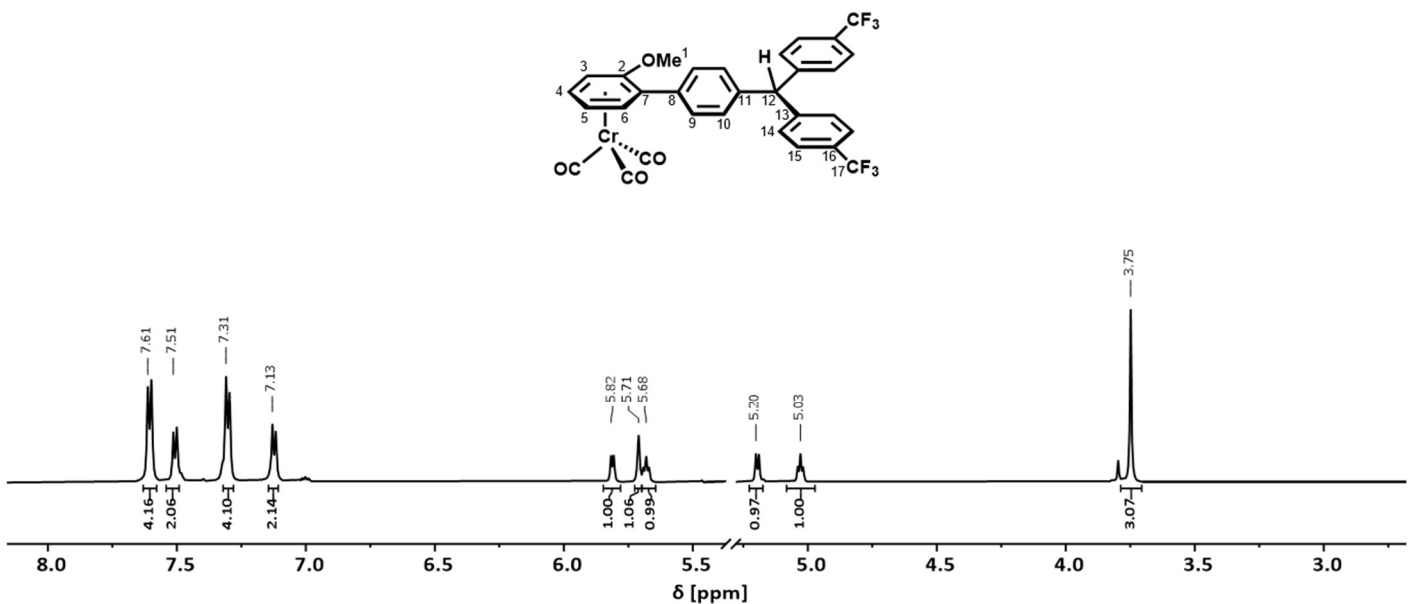
**Figure S24.** Plot of  $\Delta G$  against  $T$  for  $3^+$  with a linear regression line.



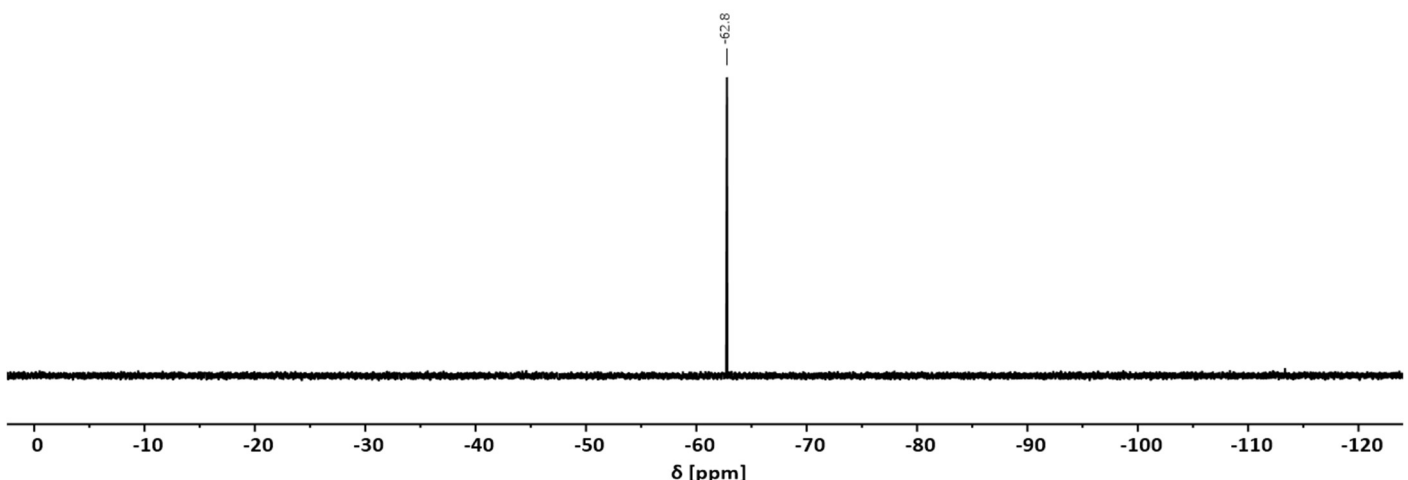
**Figure S25.** (a) EPR spectrum of  $\mathbf{1}^{+}$  in  $\text{CH}_2\text{Cl}_2$  at  $-70\text{ }^{\circ}\text{C}$  (black) and corresponding simulation (blue). (b) EPR spectra of  $\mathbf{1}^{+}$  in  $\text{CH}_2\text{Cl}_2$  at temperatures between  $-90$  and  $-40\text{ }^{\circ}\text{C}$ . (c) EPR spectrum of  $\mathbf{1}^{+}$  at  $-70$  after warming to  $-40\text{ }^{\circ}\text{C}$ . (d) EPR spectrum of  $\mathbf{1}^{+}$  in frozen  $\text{CH}_2\text{Cl}_2$  at  $77\text{ K}$ .



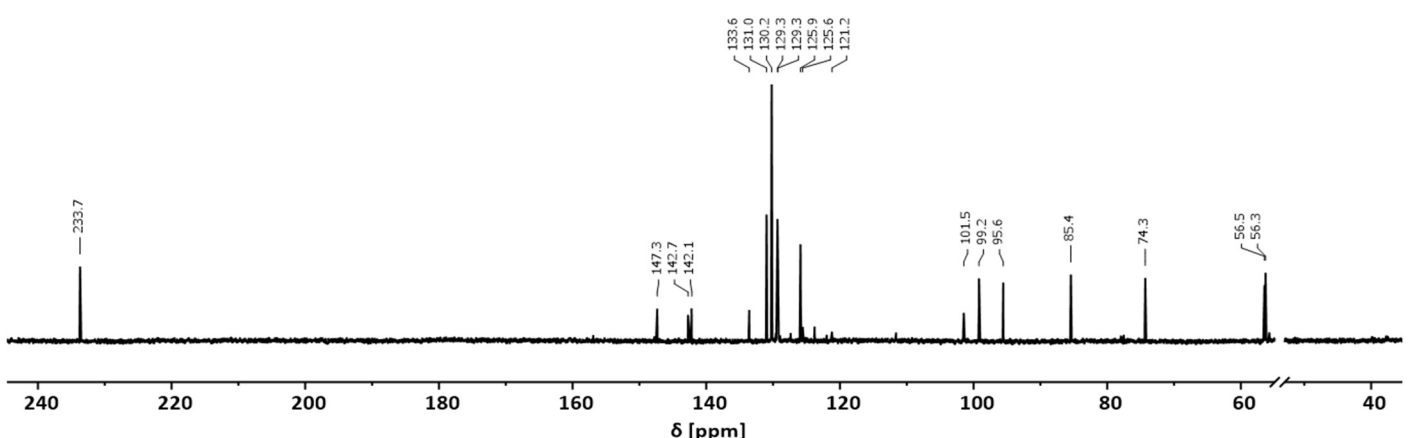
**Figure S26.** EPR spectra of  $\mathbf{3}^{+}$  in  $\text{CH}_2\text{Cl}_2$  at  $-40\text{ }^{\circ}\text{C}$  (black) and at  $-70$  after warming to  $-40\text{ }^{\circ}\text{C}$  (blue).



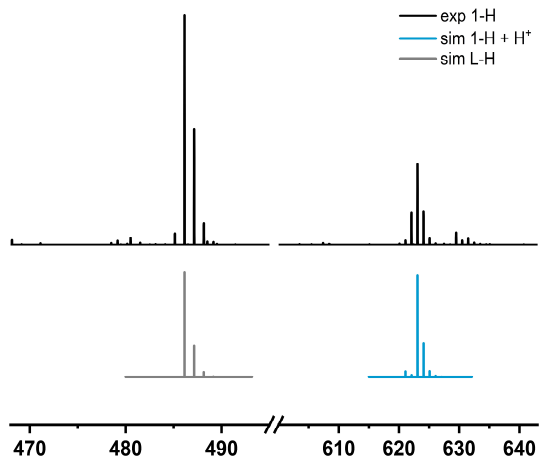
**Figure S27.** <sup>1</sup>H-NMR spectrum of complex **1-H** (600 MHz, CD<sub>2</sub>Cl<sub>2</sub>).



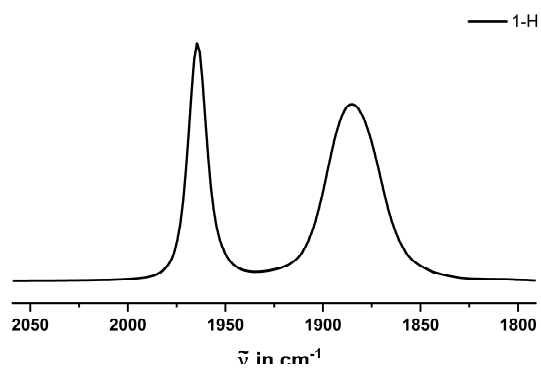
**Figure S28.** <sup>19</sup>F{<sup>1</sup>H}-NMR spectrum of complex **1-H** (376 MHz, CD<sub>2</sub>Cl<sub>2</sub>).



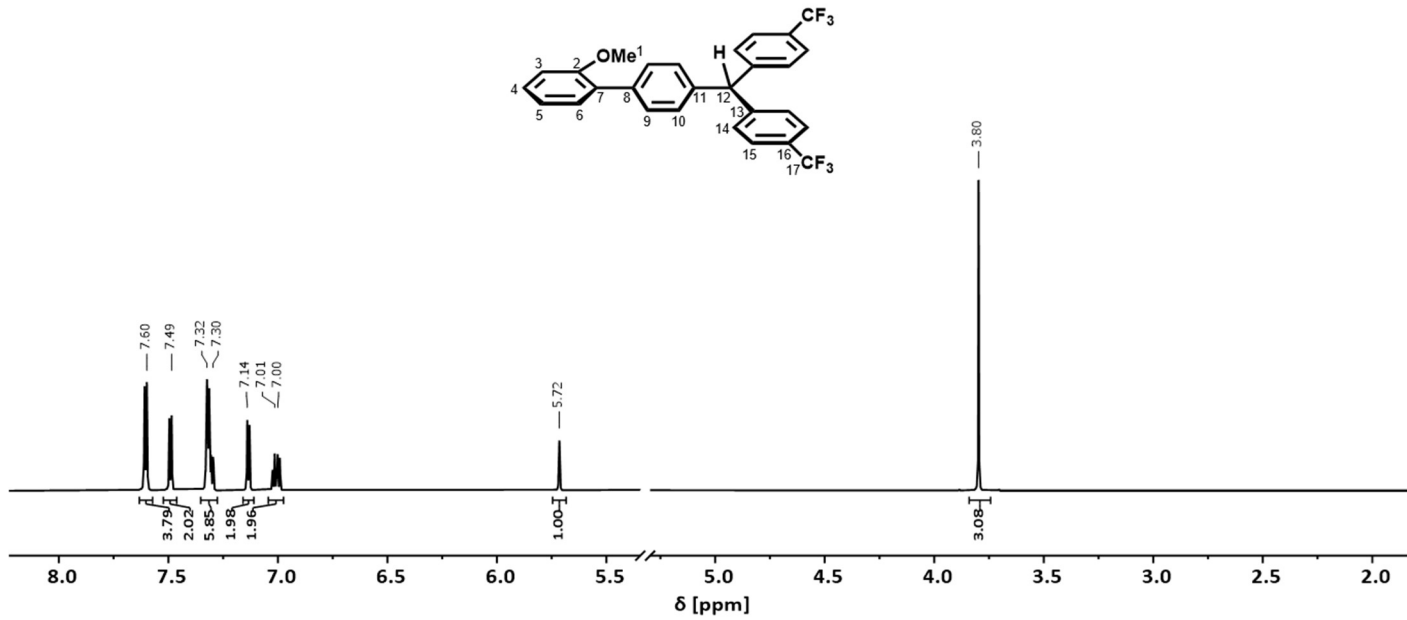
**Figure S29.** <sup>13</sup>C{<sup>1</sup>H}-NMR spectrum of complex **1-H** (151 MHz, CD<sub>2</sub>Cl<sub>2</sub>).



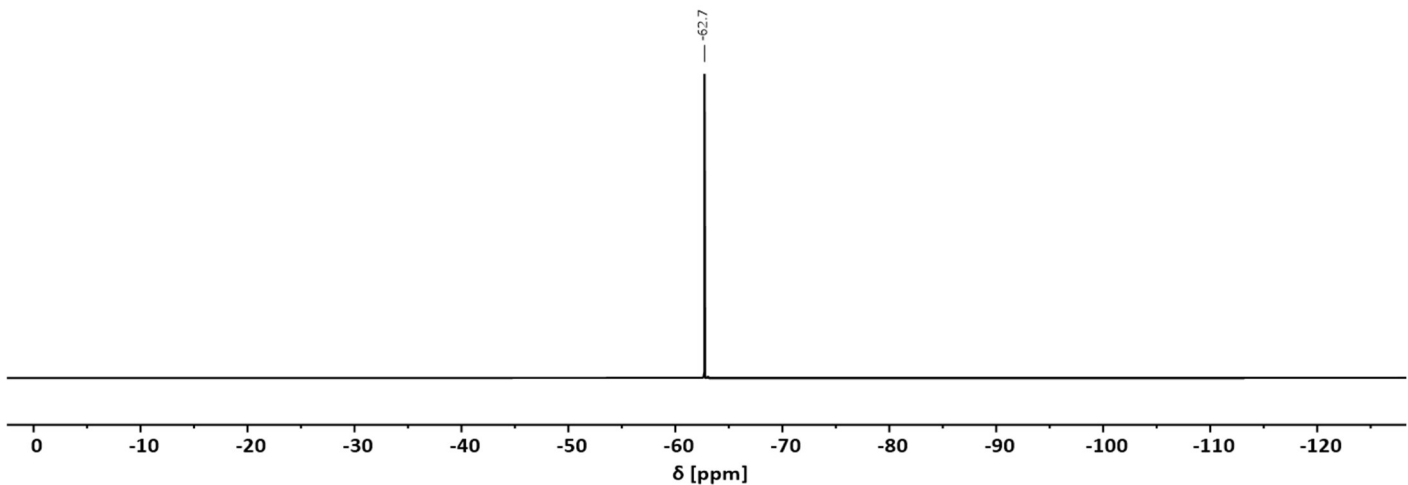
**Figure S30.** Experimental (black) and simulated (**1-H** + H<sup>+</sup> blue, **L-H** grey) mass spectrum of complex **1-H**.



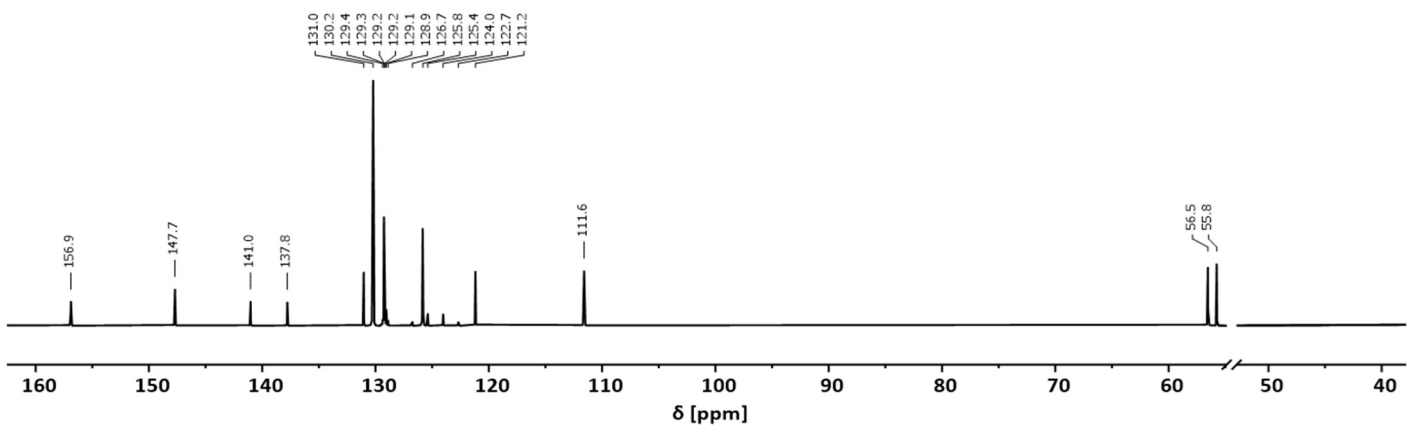
**Figure S31.** Carbonyl-region of the IR spectrum of complex **1-H** in  $\text{CH}_2\text{Cl}_2$ .



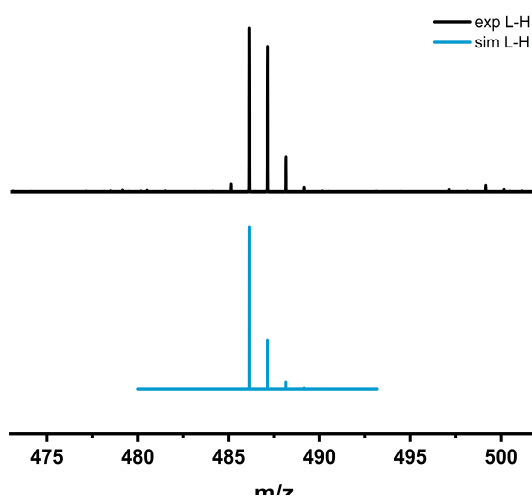
**Figure S32.** <sup>1</sup>H-NMR spectrum of **L-H** (800 MHz,  $\text{CD}_2\text{Cl}_2$ ).



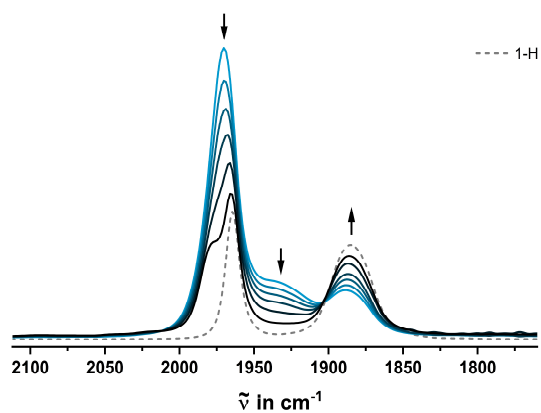
**Figure S33.**  $^{19}\text{F}\{^1\text{H}\}$ -NMR spectrum of **L-H** (752 MHz,  $\text{CD}_2\text{Cl}_2$ ).



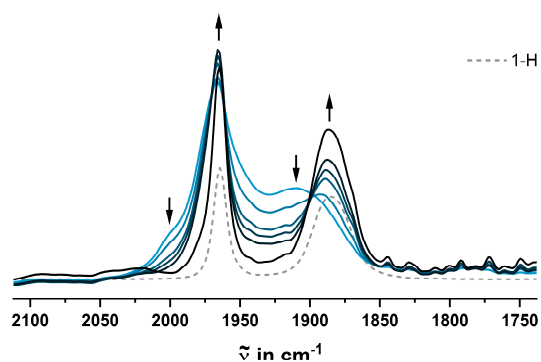
**Figure S34.**  $^{13}\text{C}\{^1\text{H}\}$ -NMR spectrum of **L-H** (202 MHz,  $\text{CD}_2\text{Cl}_2$ ).



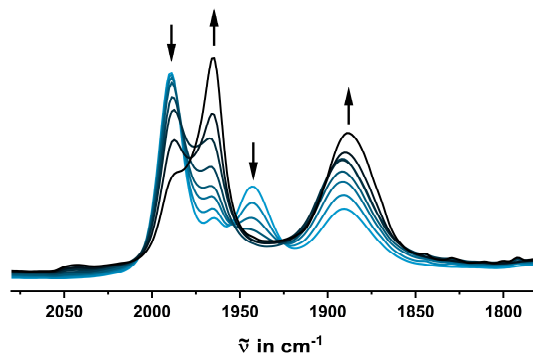
**Figure S35.** Experimental (black) and simulated (blue) mass spectrum of **L-H**.



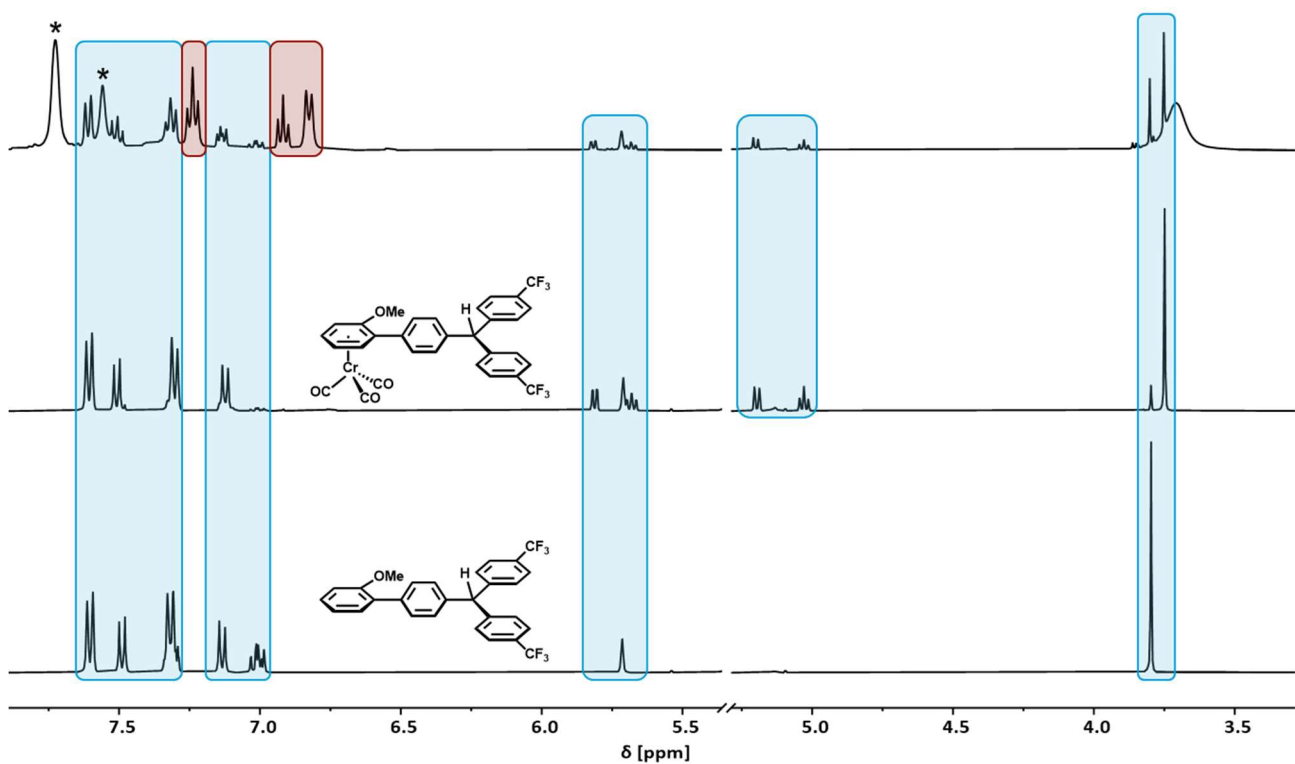
**Figure S36.** IR spectra recorded during decomposition of  $\mathbf{1}^+$  at r.t. The grey broken line represents the IR spectrum of complex  $\mathbf{1}\text{-H}$ .



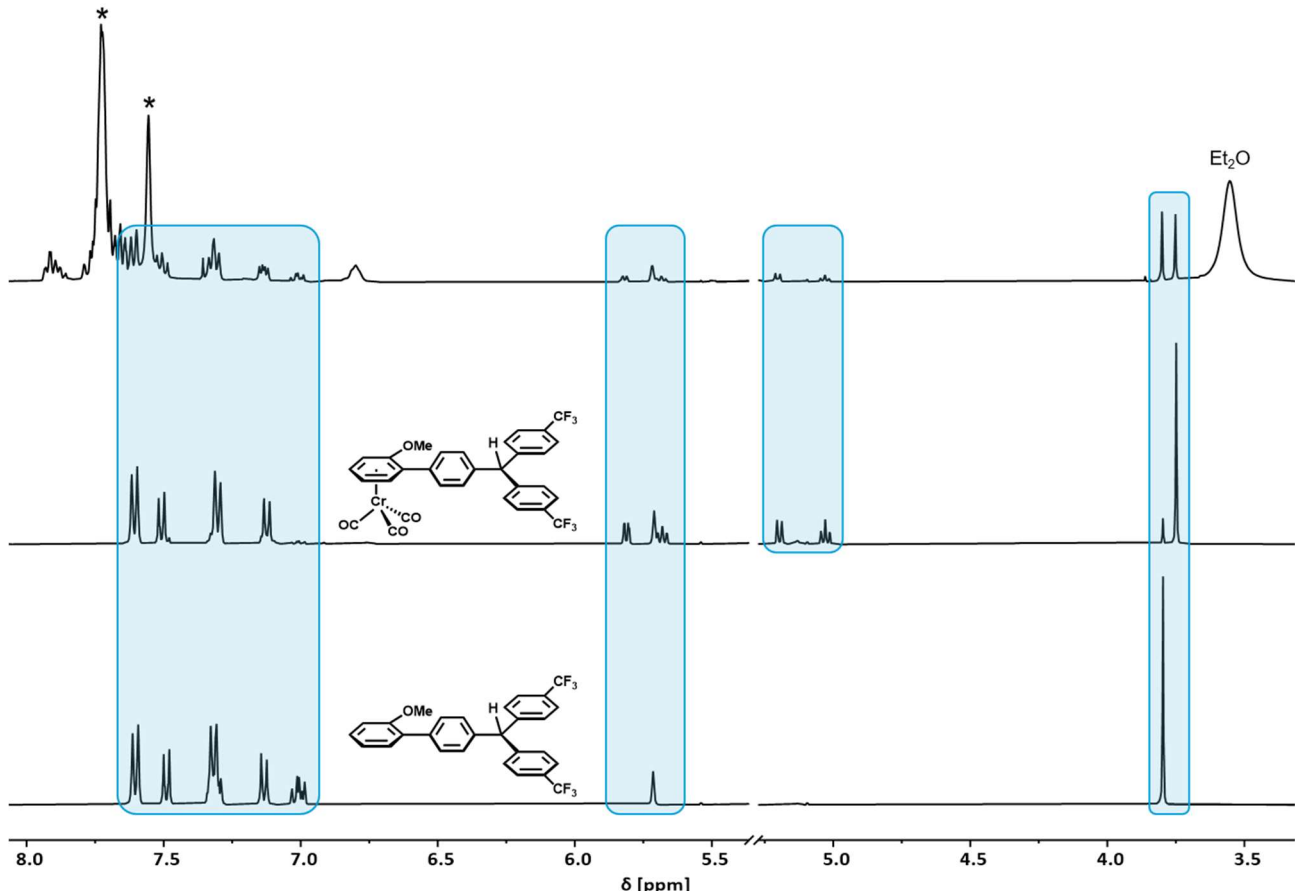
**Figure S37.** IR spectra recorded during decomposition of  $\mathbf{2}^+$  at r.t. The grey broken line represents the IR spectrum of complex  $\mathbf{1}\text{-H}$ .



**Figure S38.** IR spectra recorded during decomposition of  $\mathbf{3}^+$  at r.t.



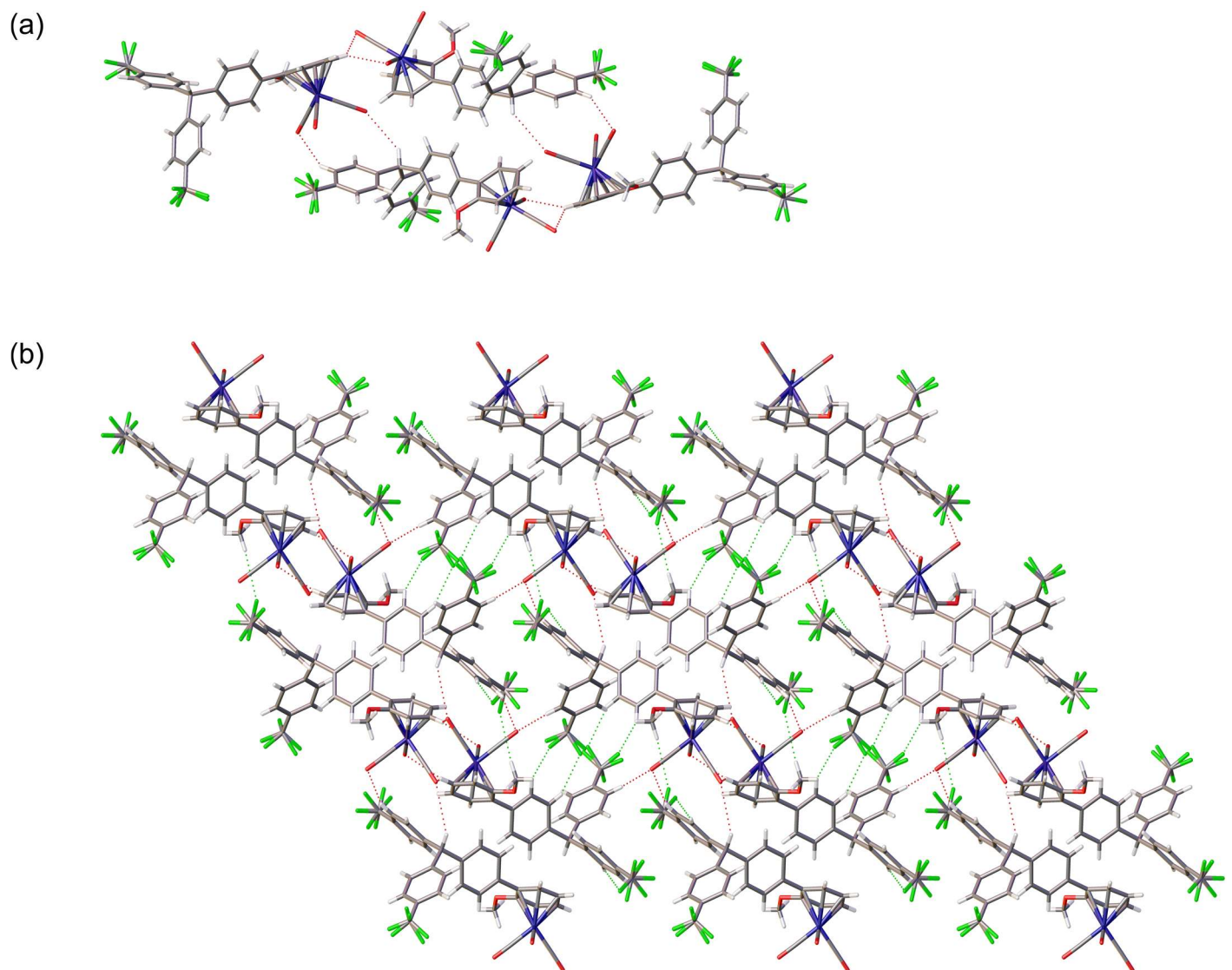
**Figure S39.** <sup>1</sup>H-NMR spectra of **2<sup>+</sup>** (top, 12 h after addition of Brookhart's acid at r.t.) and its decomposition products **1-H** (middle) and **L-H** (bottom) (400 MHz, CD<sub>2</sub>Cl<sub>2</sub>). [BAr<sup>F<sub>24</sub></sup>]<sup>-</sup> signals are marked with asterisks. The signals marked in red could be assigned to phenol.



**Figure S40.** <sup>1</sup>H-NMR spectra of **2<sup>+</sup>** (top, 12 h after addition of Brookhart's acid at r.t.) and its decomposition products **1-H** (middle) and **L-H** (bottom) (400 MHz, CD<sub>2</sub>Cl<sub>2</sub>). [BAr<sup>F<sub>24</sub></sup>]<sup>-</sup> signals are marked with asterisks.

**Table S3.** Crystal data and structure refinement for complex **1-H**.

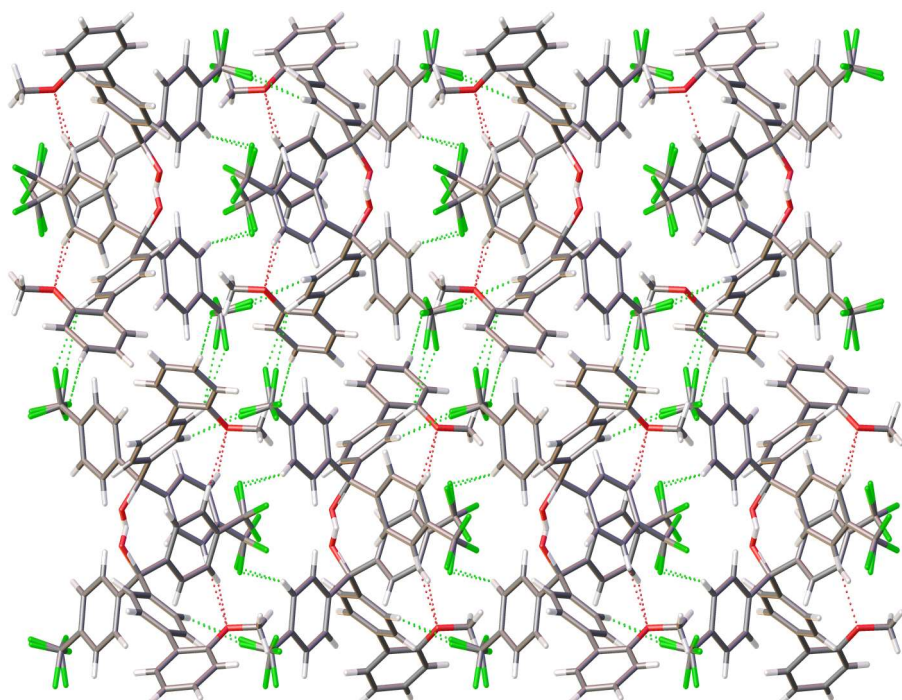
Empirical formula	C <sub>31</sub> H <sub>20</sub> CrF <sub>6</sub> O <sub>4</sub>
Formula weight	622.47
Temperature / K	100
Crystal system	monoclinic
Space group	P2 <sub>1</sub> /n
a / Å	17.2787(10)
b / Å	7.6071(6)
c / Å	20.5128(12)
α / °	90
β / °	95.142(5)
γ / °	90
Volume / Å <sup>3</sup>	2685.4(3)
Z	4
ρ <sub>calcg</sub> / cm <sup>3</sup>	1.540
μ / mm <sup>-1</sup>	4.216
F(000)	1264.0
Crystal size / mm <sup>3</sup>	0.17 × 0.068 × 0.015
Radiation	Cu Kα ( $\lambda = 1.54186$ )
2Θ range for data collection / °	6.412 to 132.054
Index ranges	-20 ≤ h ≤ 20, -8 ≤ k ≤ 7, -24 ≤ l ≤ 19
Reflections collected	12293
Independent reflections	4489 [R <sub>int</sub> = 0.1260, R <sub>sigma</sub> = 0.1315]
Data/restraints/parameters	4489/78/437
Goodness-of-fit on F <sup>2</sup>	1.189
Final R indexes [I ≥ 2σ (I)]	R <sub>1</sub> = 0.1280, wR <sub>2</sub> = 0.3053
Final R indexes [all data]	R <sub>1</sub> = 0.2236, wR <sub>2</sub> = 0.3873
Largest diff. peak/hole / e Å <sup>-3</sup>	1.45/-0.93



**Figure S41.** (a) Packing of two  $R_p$  and  $S_p$  enantiomers each of **1-H** within the unit cell. (b) Packing of the units; view along the  $b$  axis. Short contacts are indicated by red broken lines.

**Table S4.** Crystal data and structure refinement for L-H.

Empirical formula	C <sub>28</sub> H <sub>20</sub> F <sub>6</sub> O <sub>1.04</sub>
Formula weight	487.08
Temperature / K	100
Crystal system	orthorhombic
Space group	Pbca
a / Å	9.6538(4)
b / Å	18.3824(6)
c / Å	25.4401(7)
α / °	90
β / °	90
γ / °	90
Volume / Å <sup>3</sup>	4514.6(3)
Z	8
$\rho_{\text{calcd}}$ g / cm <sup>3</sup>	1.433
$\mu$ / mm <sup>-1</sup>	0.120
F(000)	2003.0
Crystal size / mm <sup>3</sup>	0.3 × 0.25 × 0.2
Radiation	Mo K $\alpha$ ( $\lambda = 0.71073$ )
2 $\Theta$ range for data collection / °	5.028 to 55.118
Index ranges	-12 ≤ h ≤ 12, -23 ≤ k ≤ 22, -33 ≤ l ≤ 30
Reflections collected	17345
Independent reflections	5176 [ $R_{\text{int}} = 0.0228$ , $R_{\text{sigma}} = 0.0206$ ]
Data/restraints/parameters	5176/62/375
Goodness-of-fit on $F^2$	1.103
Final R indexes [ $I \geq 2\sigma (I)$ ]	$R_1 = 0.0415$ , $wR_2 = 0.0905$
Final R indexes [all data]	$R_1 = 0.0611$ , $wR_2 = 0.1088$
Largest diff. peak/hole / e Å <sup>-3</sup>	0.29/-0.23

**Figure S42.** Packing of L-H; view along the a axis.

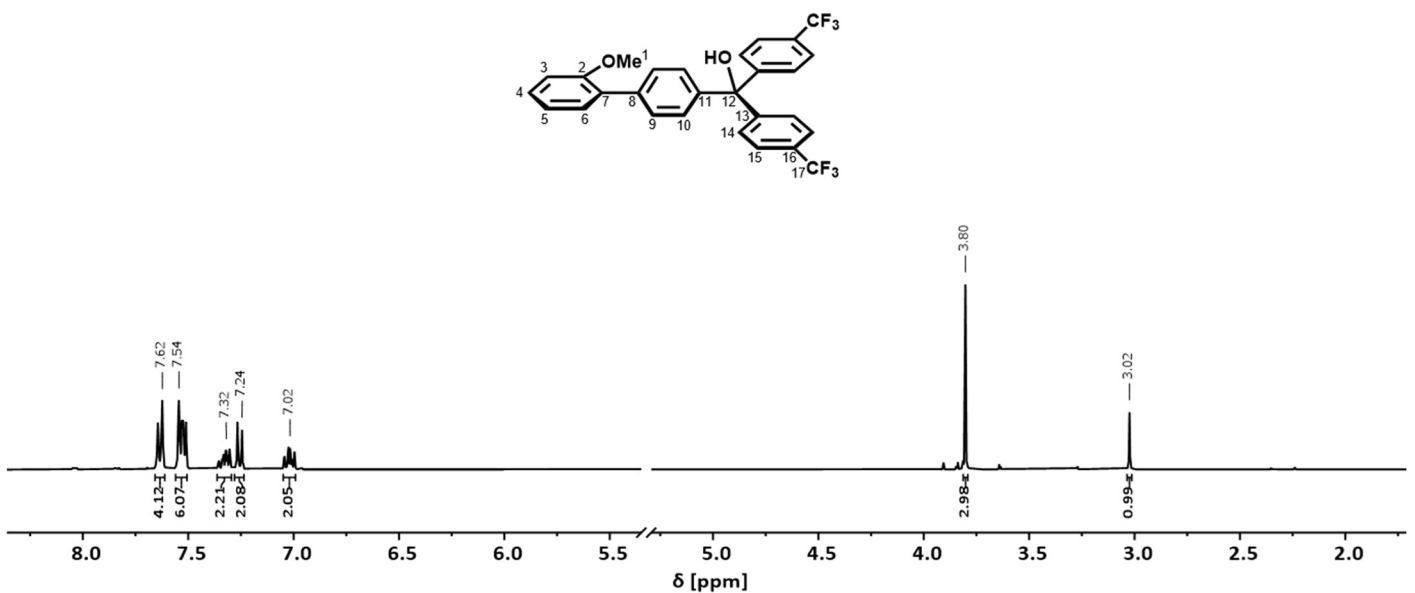


**Figure S43.**  $^1\text{H}$ -NMR spectrum of L-OH (400 MHz,  $\text{CD}_2\text{Cl}_2$ ).

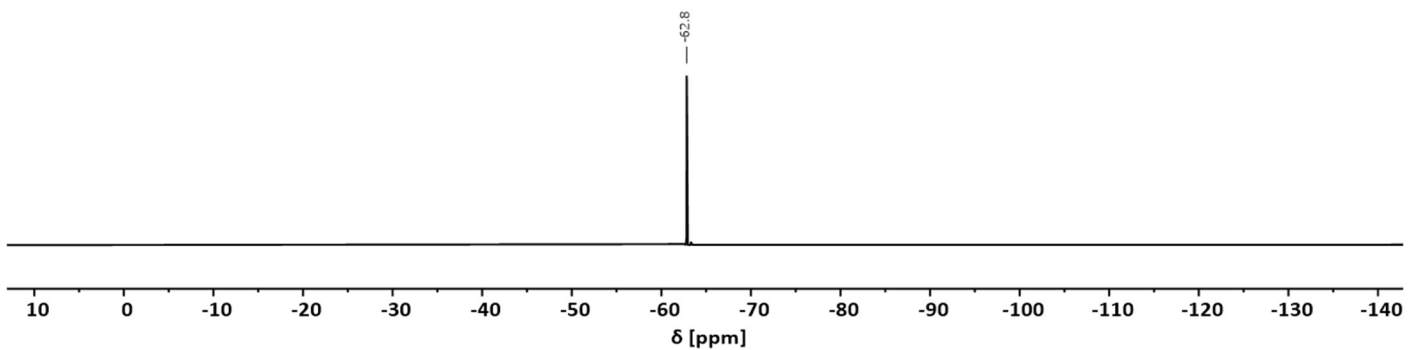


**Figure S44.**  $^{19}\text{F}\{\text{H}\}$ -NMR spectrum of L-OH (376 MHz,  $\text{CD}_2\text{Cl}_2$ ).

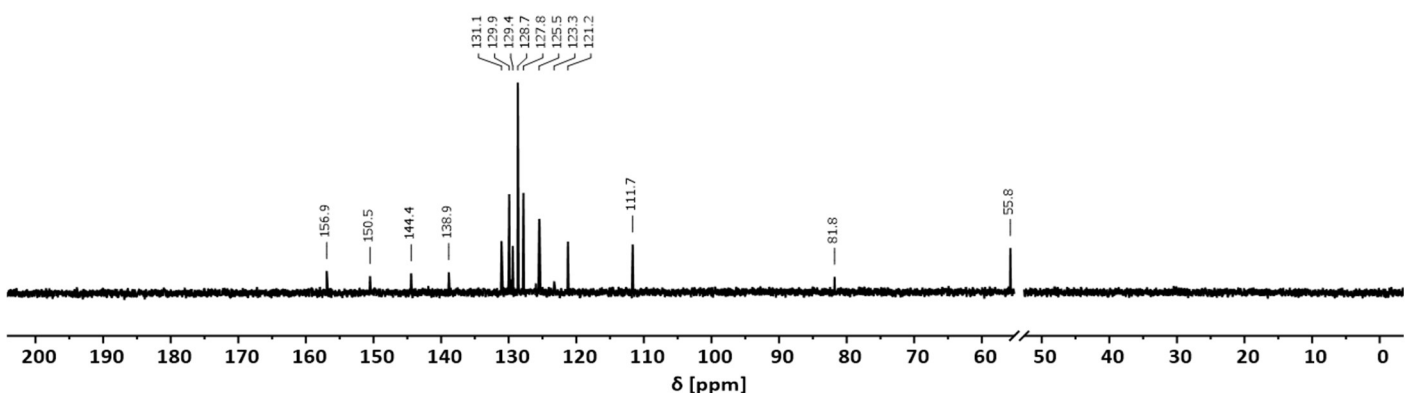


**Figure S45.**  $^{13}\text{C}\{\text{H}\}$ -NMR spectrum of L-OH (101 MHz,  $\text{CD}_2\text{Cl}_2$ ).

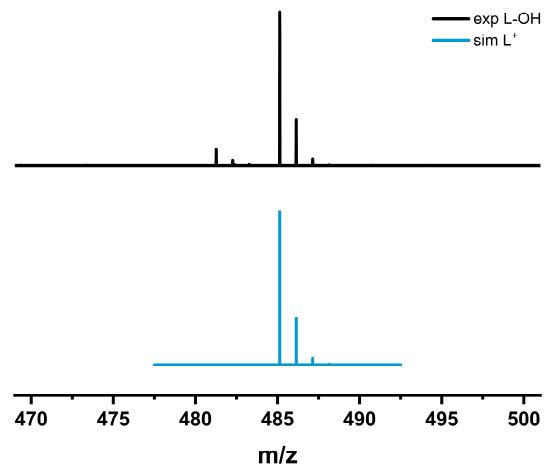


**Figure S46.** Experimental (black) and simulated (blue) mass spectrum of L-OH.